Hyperfine Interact (2011) 202:63–71
DOI 10.1007/s10751-011-0339-z

Design and construction of an electromechanical velocity modulator for Mössbauer spectroscopy

A. A. Velásquez · A. Carmona · D. Velásquez · L. Ángel

Published online: 25 August 2011

Abstract In this paper we report the design, construction and characterization of an electromechanical velocity modulator for application in Mössbauer spectroscopy. The modulator was constructed with copper coils, Neodymium magnets, steel cores and polymeric membranes. The magnetic field in the driving and velocity sensing stages was analyzed by the finite element method, which showed a linear relation between the magnetic field in the region of motion of both coils and the position of the coils within the steel cores. The results obtained by computational simulation allowed us to optimize geometries and dimensions of the elements of the system. The modulator presented its first resonance frequency at 16.7 Hz, this value was in good agreement with that predicted by a second order model, which showed a resonant frequency of 16.8 Hz. The linearity of the velocity signal of the modulator was analyzed through an optical method, based on a Michelson–Morley interferometer, in which the modulator moved one of the mirrors. Results showed a satisfactory linearity of the velocity signal obtained in the sensing coil, whose correlation with a straight line was around 0.99987 for a triangular reference waveform.

Keywords Mössbauer spectroscopy · Velocity modulator · Finite element method · Optical calibration

A. A. Velásquez (✉) · A. Carmona
Grupo de Electromagnetismo Aplicado,
Universidad EAFIT, A.A 3300, Medellín, Colombia
e-mail: avelas26@eafit.edu.co

D. Velásquez · L. Ángel
Grupo de Óptica Aplicada, Universidad EAFIT,
A.A 3300, Medellín, Colombia

1 Introduction

One of the main components of any Mössbauer spectrometer is the velocity modulator, which moves the radioactive source with a controlled velocity in order to produce the Doppler change in the energy of the gamma rays, required to achieve the resonance with the nuclear states of Mössbauer isotopes present in the absorber. Some types of modulators have been reported in the literature, among them is the Doppler modulator system developed by Kankeleit [1], which is based on applied concepts of the electromagnetic theory, namely: Lorentz force for the driving coil and the Faraday's induction law for the velocity sensing coil. A more recent modulator, built with a piezoelectric actuator was developed by Molins et al. [2], whose main advantage is its small size, close to 3 cm, which gives the possibility to introduce the Mössbauer source and the absorber inside a cryostat when a low temperature measure is necessary, allowing to obtain better counting rates than those obtained when the source and absorber are located in opposite sides of the cryostat window. There are also some commercial electromechanical modulators such as the early model A.S.A K-3 Linear Motor developed by Austin Sciences Associates [3], the models MA-260, MA-260S and MVT-1000, developed by Wissel GmbH [4], the electromechanical transducer and sensing system of the MsAa-3 RENON Mössbauer Spectrometer [5]. Other important design to mention is the velocity modulator present in the mini spectrometer MIMOS II, sent to Mars in 2003, as one of the instruments of the Spirit and Opportunity robots, which is based on the electromechanical design proposed by Kankeleit [6]. This modulator moves two ^{57}Co sources, one of which is used for calibration of the Mössbauer spectrometer and the other is used to irradiate the samples present in rocks and soils. The success of the mission of MIMOS II in the Mars exploration evidences the convenience of the electromechanical systems for exigent operation conditions, including field applications for in situ analysis. No much information additional to the above mentioned about velocity modulators for Mössbauer spectroscopy is available, however electromechanical designs seem to be most popular due to its simple and stable architecture and known mathematic model, which can be well approximate for a second order system [7]. Taking in account the importance for developing functional and low cost systems, useful to make investigation in material science, we report in this article the design and construction of an electromechanical velocity modulator for Mössbauer spectroscopy, which incorporates some advantages of the rare earth magnets (NdFeB), such as its high BH product compared with that of AlNiCo and CuNiFe magnets of comparable dimensions, as well as functional, reproducible and low cost elements for the oscillating structure. The behavior of the magnetic field within the steel cores was simulated by the finite element method in order to test the linearity of the driving and sensing stages. The process of the design and characterization of the velocity modulator is described through this paper.

2 Design of the prototype

2.1 Internal architecture

The starting point of our design was the model reported by Kankeleit [1], which constitutes the basis for most electromechanical modulators reported in the literature.

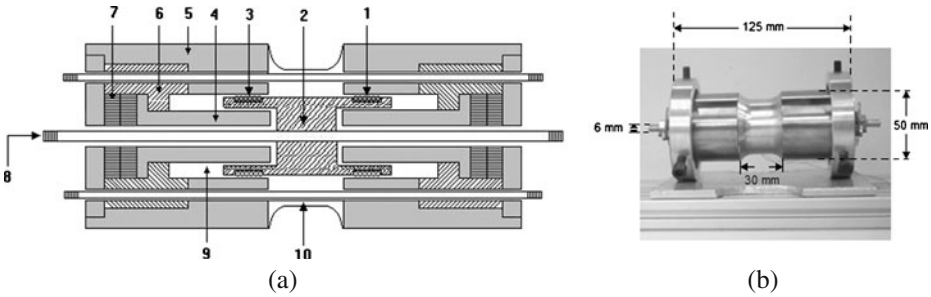

Fig. 1 **a** Velocity modulator scheme: *1* sensing coil, *2* nylon support, *3* driving coil, *4* internal core, *5* external core, *6* aluminum bushing, *7* NdFeB magnets, *8* aluminum rod, *9* air cavity for the coil motion and *10* aluminum coupling housing, **b** View of the prototype

This design is based on a symmetrical structure of loudspeaker type, in which the actuator (driving stage) and the sensing stage (velocity stage) are similar and they are located in opposite ends of the structure. The main difference between driving and sensing stages is the electrical resistance of the coils, which is of the order of 1 Ω for the driving coil and 100 Ω for the sensing coil. Each coil moves through a steel core with cylindrical shape, which is magnetized by permanent magnets located concentrically with the core. The magnetic permeability of the steel core increases the intensity of the magnetic field $\boldsymbol{B}$ through the coils and gives a definite direction and magnitude to the magnetic field which crosses them. We used NdFeB magnets with disc shape, this choice obeys to the fact that the high product $\boldsymbol{BH}$ of this material gives us a magnetic field higher than that obtained with CuNiFe, AlNiCo and SmCo magnets of comparable dimensions [8], allowing to have a low current consumption for having a reasonable magnetic force on the driving coil, a convenient signal to noise ratio in the velocity sensing coil and a low size design.

2.2 Driving and sensing coils

The Fig. 1 presents the scheme and the external view of the velocity modulator. The oscillating structure is composed by driving and sensing coils as well as a cylindrical nylon support used for winding both coils. The driving coil was made with 120 turns of copper wire, reference AWG 36, which was wound onto an end of a nylon cylinder with thickness 2 mm. The sensing coil was made with 500 turns of copper wire, reference AWG 42. The electrical resistances of the driving and sensing coils were (8.6 ± 0.1) Ω and (250.4 ± 0.1) Ω respectively. Both coils oscillate inside an air cavity surrounded by an internal steel core and an external steel core, this last also serves as housing of the structure.

2.3 Driving and sensing cores

The architecture of driving and sensing cores is also sketched in Fig. 1a. Both structures are identical, they are composed of a solid axis of steel, reference ASI-SAE 1020, centered on a cylindrical cavity of the same material. An aluminum bushing was employed in order to keep concentric both steel structures, as well as to align the NdFeB magnets with the inner core. To analyze the linearity between the position

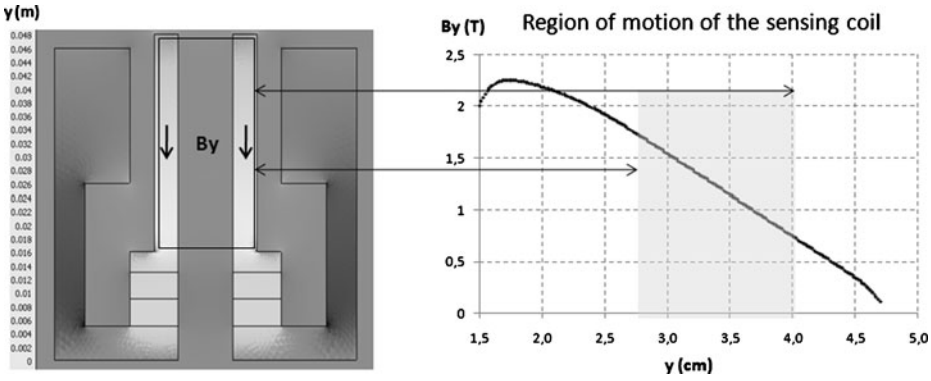

Fig. 2 **a** Region of the sensing core where the magnetic field B is calculated, **b** Relation between the magnetic field B and the position y parallel to the steel core axis

of each coil and the magnetic flux $\boldsymbol{\phi_B}$ which crosses it, the magnetic field within the cores was simulated by the finite element method [9, 10]. This method calculates the magnetic field $\boldsymbol{B}$ in the region where the coil moves, limited by the boundary conditions imposed by us. In our case, the region of interest was a cylinder of 3 cm of length and 2 cm of diameter, which represents the portion of the internal core where the motion of the coils takes place. A view of the cross section where the magnetic field was calculated is presented in Fig. 2. The sensing coil moves in the interval [2.7, 4.0] cm, where the magnetic field $\boldsymbol{B}$ varies linearly with the y coordinate. A linear relation between $\boldsymbol{B}$ and $\boldsymbol{y}$ produces a linear relation between the voltage induced in the sensing coil, $V(t)$, and the instantaneous velocity $v(t)$ of this coil according to the Faraday's law:

$$V(t) = \alpha \frac{d\phi_B}{dt} = \alpha \frac{d(\beta y)}{dt} = \alpha\beta \frac{dy}{dt} = \delta v(t) \tag{1}$$

Where δ is the sensibility of the sensing coil, which depends on parameters such as its area, the number of turns and the magnetic properties of the core.

In the driving stage the force responsible for the oscillation of the moving structure is that due to the radial component of the magnetic field present in the air gap between the internal and the external cores. To analyze the linearity of this force with the current in the driving coil, the behavior of the radial component of the magnetic field in the air gap was also analyzed by the finite element method; the results are presented in Fig. 3. The component B_r varied less than 1% in the interval $y \in [2.7, 4.0]$ cm, where the driving coil motion takes place, this behavior gives a linear relation between the magnetic force resulting on the driving coil and the current flowing through it.

2.4 Permanent magnets

Permanent magnets of NdFeB with energy density $(\mathrm{BH})_{\max} = 35$ MGOe and Curie temperature of 553 K were used in our design. The magnets have ring shape with

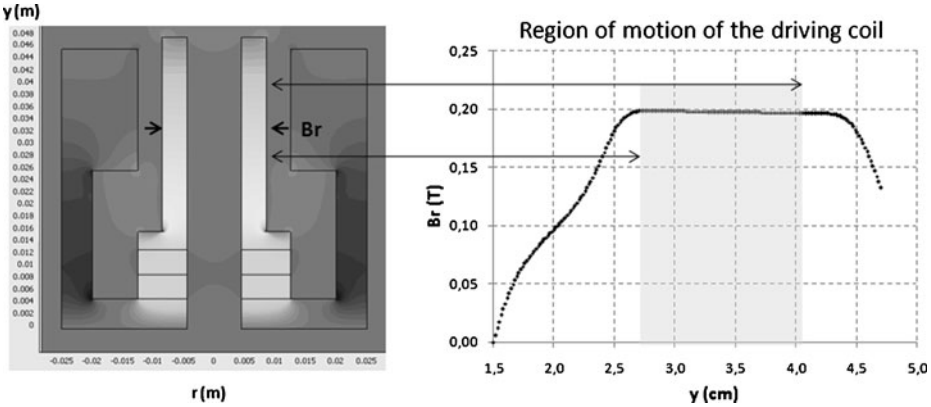

Fig. 3 **a** Region of the driving core where the radial component B_r of the magnetic field is calculated, **b** relation between B_r and the position y

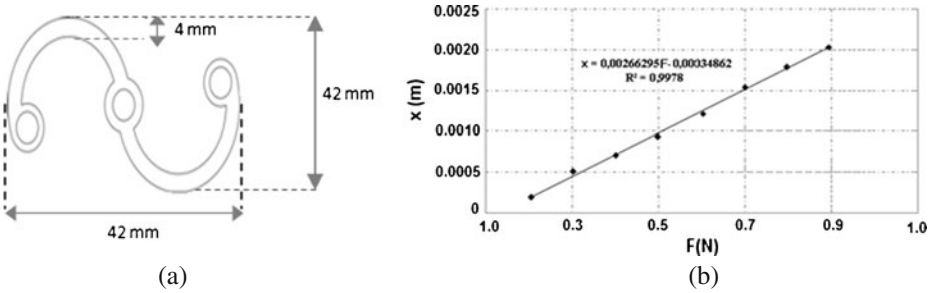

Fig. 4 **a** Design of the polymeric membranes for the sustentation system of the oscillating structure, **b** elongation of the membranes vs. force applied to the aluminum rod

25 mm of outer diameter, 9 mm of inner diameter and 4 mm of thickness. The magnetic induction field had its maximal value of 0.24 T in the center of the magnet, which was measured with a teslameter PHYWE with an axial Hallsonde series 13610.01.

2.5 Polymeric membranes

The Fig. 4a presents the scheme of the elastic membranes used for the sustentation of the oscillating structure. The membranes were made of polyethylene terephthalate, with thickness 0.5 mm and density 1.425 g/cm^3.

The elastic constant of the membranes system was measured through a mechanical experiment, in which a variable mass was suspended of the lower end of a thread while the upper end of the thread was attached to one end of the aluminum rod. The small displacements of the rod were measured with a microscope. Data of rod displacement vs. applied force are presented in Fig. 4b. A linear fitting of the

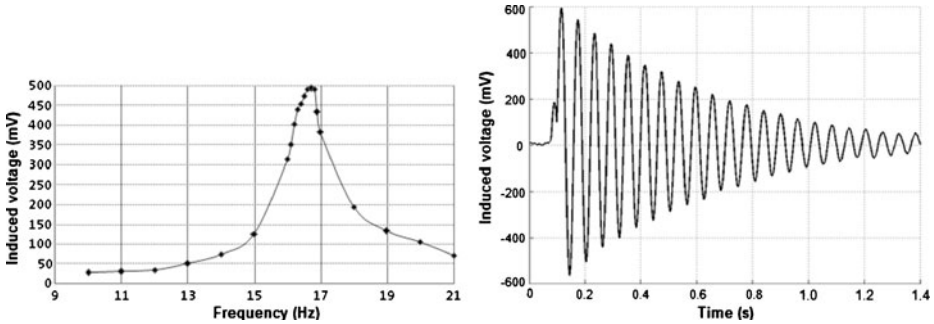

(a) (b)

Fig. 5 **a** Frequency response of the velocity modulator, **b** impulse response

experimental data gave the value $k_1+k_2 = (376 \pm 4)$ N/m for the elastic constant of the membranes system.

3 Characterization of the velocity modulator

3.1 Resonance frequency

Resonance frequency of the modulator was measured by stimulating the driving coil with a sinusoidal signal with 50 mV of amplitude, provided by a wave generator Agilent 33220A-20 MHz. The signal induced in the sensing coil was recorded with a digital storage oscilloscope Tektronicx TDS 3052B-500 MHz. The graph of amplitude of the signal induced in the sensing coil vs. frequency of the stimulus signal is presented in Fig. 5a, from this graph a resonance frequency of 16.7 Hz was found.

3.2 Impulse response

In order to have an idea of the mathematical model of the velocity modulator in terms of its transference function, a mechanical impulse was given to the system, which consisted in a brief shove on the aluminum rod. The signal induced in the sensing coil was recorded with the storage oscilloscope and presented in Fig. 5b, the response obtained was characteristic of a second order system with a damping term. According to the impulse response function, the mathematical model of the system can be approximate by the equation:

$$m\frac{d^2x}{dt^2} + b\frac{dx}{dt} + (k_1 + k_2)\,x = f\,(t) \tag{2}$$

Where $m = (33.6 \pm 0.1)$ g is the mass of the oscillating structure, b is the damping parameter; $k_1 + k_2$ is the elastic constant of the membranes system and $f(t)$ is the impulsive force communicated to the rod. The damping parameter b was estimated from the equation of the envelope of the oscillating signal presented in Fig. 5b. The envelope was well fitted by an exponential decreasing function, from which the value

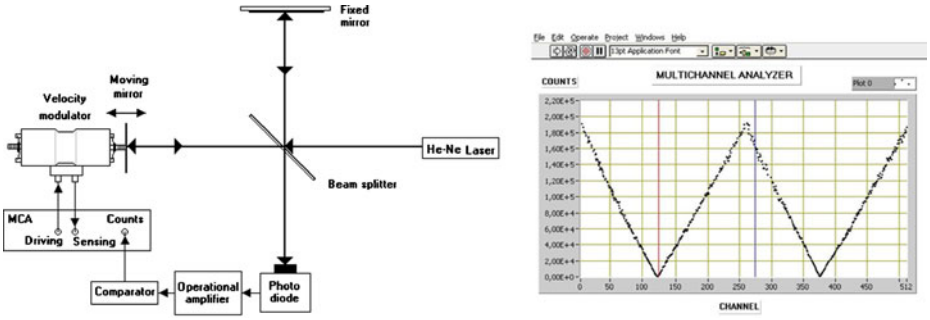

Fig. 6 **a** Scheme of the Michelson–Morley interferometer used to measure the velocity signal of the modulator, **b** Number of counts vs. channel registered by the multichannel analyzer

$b = (0.296 \pm 0.004)$ kgs^{-1} was obtained. According to the mathematical model (2) the resonance frequency of the system is $f_R = (16.8 \pm 0.1)$ Hz. The discrepancy between the measured resonance frequency and the frequency predicted by the mathematical model is 0.6%, which shows that the velocity modulator can be well described by a second order linear system.

3.3 Linearity of the velocity signal

The linearity of the velocity modulator was analyzed through an absolute velocity calibration method, which has been reported in the literature [11–14]. This method is based on a Michelson–Morley Interferometer, in which the first mirror is fixed to one arm of the interferometer while the second mirror is clamped to the oscillating rod of the velocity modulator. A coherent laser beam splits in two beams when it pass through a beam splitter, the first beam is directed towards the fixed mirror and the second one is directed towards the moving mirror clamped to the modulator rod. The reflected beams are again combined in the beam splitter and its interference pattern is observed on a screen where a photodiode is located. The rings of the pattern alternate their intensity when the mirror moves a length of $\lambda/4$, being λ the wavelength of laser light used. The rod of the modulator oscillated according to a triangular reference signal of 6 Hz and 512 channels programmed in our multichannel analyzer (MCA). The basic architecture of the interferometer is schematized in Fig. 6a. For the experiment we used a He–Ne laser with 20 mW of power and $\lambda = 632.8$ nm, a beam splitter cube with 50%–50% transmitted intensity, a fixed mirror with $\lambda/4$ flatness, a photodiode ODD-660W with 1 ns of response time and spectral sensibility bandwidth 600–700 nm, and a counting fringe system designed in our laboratory.

The photodiode was located in the center of the pattern and the pulses detected were converted to logical TTL pulses through a voltage comparator circuit based on a high speed operational amplifier AD8051 with 110 MHz bandwidth and 145 V/μs slew rate. Logical pulses were sent to the counting module of the multichannel analyzer, which stored the counts produced in each channel of the reference velocity signal of the velocity modulator. The graph of the counts vs. channel in which they are registered is presented in Fig. 6b. A linear fit of the data in the interval of channels

128–256 showed a correlation coefficient $R^2 = 0.99987$. The fitting of the data in the interval of channels 256–384 showed a correlation coefficient $R^2 = 0.99985$. From the graph, the magnitude of the velocity of the oscillating structure in the velocity channel *i* can be obtained from the equation [11]:

$$v_i = \frac{\lambda N_i}{2nt_{dwell}} \tag{3}$$

Where λ is the wavelength of the laser light used, N_i is the average number of logical pulses per cycle registered by the MCA in the channel *i*, *n*is the refraction index of the media and t_{dwell} is the time interval during which the counts are stored for each channel of the reference signal. The parameters of our experiment were: $\lambda = 632.8$ nm, $n \approx 1.0$ and $t_{dwell} = (162.0 \pm 0.5)$ μs. Counts were registered for a time of 100 min, during this time 197,010 pulses were registered in the channel 256, giving an average value $N_{256} = 5.5$. With these parameters we obtained v = (10.69 ± 0.01) mm/s, which is the maximal velocity of the modulator for the conditions of the experiment.

4 Conclusions

We have designed a velocity modulator apt for use in Mössbauer spectroscopy, whose linearity deviation was better than 0.02% over a velocity scale range from −10.69 mm/s to 10.69 mm/s, for a triangular reference signal. The system implements very functional, accessible and reproducible components, such as Neodymium magnets, polymeric membranes, copper coils and steel cores. The simulation of the system by the finite element method allowed us to find convenient geometries and dimensions for steel cores, magnets and coils in order to have a linear response of the driving and sensing stages of the velocity modulator. The system was well described by a linear second order mathematical model, with a resonance frequency of (16.7 ± 0.1) Hz. The presented design is an attractive choice for the users of the Mössbauer spectroscopy technique, who are interested in the design and construction of functional and low cost instrumentation system for their laboratories.

References

1. Kankeleit, E.: Feedback in electromechanical drive system. Mössbauer Eff. Methodol. **1**, 47 (1965)
2. Casas, L.L., Molins, E., Roig, A.: Miniaturization of a Mössbauer spectrometer using a piezo-transducer and a solid state detector. Hyperfine Interact. **141/142**, 125 (2002)
3. Austin Science Associates, Inc, A.S.A Mössbauer spectrometer: K-3 linear motor, instruction manual. Austin, TX (1997)
4. Wissel. Mössbauer driving system 260: Instruction Manual. Germany (1996)
5. Górnicki, R., Blachowski, A., Ruebenbauer, K.: In: Proceedings Nukleonika, vol. 52(1), p. S7 (2007)
6. Klingelhöfer, G., Bernhardt, B., Foh, J., Bonnes, U., Rodionov, D., De Souza, P.A., Schröder, Ch., Gellert, R., Kane, S., Gütlich, P., Kankeleit, E.: The miniaturized Mössbauer spectrometer MIMOS II for extraterrestrial and outdoor terrestrial applications: a status report. Hyperfine Interact. **144/145**, 371 (2002)
7. Yadagiri Reddy, P., Narayan Reddy, P., Seshakumari, Ch., Rama Reddy, K.: On the transducer function of an electromechanical transducer an application to the Mössbauer velocity drive. Nucl. Instrum. Methods. **213**, 381–385 (1983)

8. Herbst, J.F., Croat, J.J.: Neodymium–iron–boron permanent magnets. J. Magn. Magn. Mater. **100**, 57 (1991)
9. Jianming, J.: The Finite Element Method in Electromagnetics. Wiley, New York (1993)
10. COMSOL: COMSOL Multiphysics, AC/DC Module User's Guide, Version 3.5: http://www.ewp.rpi.edu/hartford/~lemcon/Comsol_terminalvelocity.pdf. Accessed 10 Feb 2010
11. Kwater, M.: Laser calibration of the Mössbauer spectrometer velocity: improvements in design. Hyperfine Interact. **116**, 53 (1998)
12. Yoshimura, T., Syoji, Y., Wakabayashi, N.: Absolute velocity control of a Mössbauer spectrometer by utilizing a laser interferometer. J. Phys. E: Sci. Instrum. **10**, 829–833 (1977)
13. Player, M.A., Wodhams, FWD.: An improved interferometric calibrator for Mössbauer spectrometer drive systems. J. Phys. E: Sci. Instrum. **9**, 1148 (1976)
14. Vandenberghe, R.E.: Mössbauer Spectroscopy and Applications in Geology. International Training Centre for Post-Graduate Soil Scientists, p. 25. State University Gent, Belgium (1990)